J. Biochem. **138**, 27–33 (2005)
DOI: 10.1093/jb/mvi093

Role of the N-Terminal Domain of Endoinulinase from *Arthrobacter* sp. S37 in Regulation of Enzyme Catalysis

Kyoung-Yun Kim, Sangkee Rhee* and Su-Il Kim*

School of Agricultural Biotechnology and Center for Agricultural Biomaterials, Seoul National University, Seoul 151-742, Korea

Received October 18, 2004; accepted April 1, 2005

Endoinulinase from *Arthrobacter* sp. S37 (EnIA), a member of the glycoside hydrolase family 32, is unique in that, unlike other members of the family, it contains a 250-residue N-terminal domain including a "laminin-G like jelly-roll" fold. This unique N-terminal domain is here suggested to be involved in dimerization and catalysis. The essentially inactive nature of enzymes produced by N-terminal truncation (Δ15, Δ45, Δ70, and Δ250) supported the pivotal role of this unique domain in catalysis and the need for its structural integrity. Significant reductions in the enzyme efficiency (k_{cat}/K_m) were observed when mutations were introduced at highly conserved tryptophan residues (Trp75 and Trp141) in the laminin-G like jelly-roll fold, implying their involvement in catalysis. Results from size-exclusion chromatography of the native and chimeric enzymes in the presence and absence of the domain suggested that the N-terminal domain could mediate dimerization.

Key words: dimerization, endoinulinase, family 32.

Abbreviations: EnIA, endoinulinase from *Arthrobacter* sp. S37; GH, glycoside hydrolase; NTD, N-terminal domain; CFTase, cycloinulo-oligosaccharide fructanotransferase; ExIB, exoinulinase from *Bacillus* sp. snu-7; SEC, size-exclusion chromatography; CBD, carbohydrate-binding domain.

Glycosidases or *O*-glycoside hydrolases (GH, EC 3.2.1) are a superfamily of enzymes catalyzing hydrolysis of the glycosidic bond between the carbohydrate moieties of various substrates with diverse substrate specificity (*1*). Classifications using hydrophobic cluster analysis and sequence alignments have grouped the enzymes into a total of 100 different families (*2–5*). Members of family GH32, although showing high similarity in their amino acid sequences, are indeed diverse in their activities, including invertase, inulinase, levanase, sucrose:sucrose 1-fructosyl transferase and fructan fructan 1-fructosyltransferase (*5*). However, little is known about the determinants of such functional diversity.

Endoinulinase [EC 3.2.1.7] from *Arthrobacter* sp. S37 (EnIA), a member of family GH32, hydrolyzes a linear polymeric carbohydrate inulin (Glucose-Fructose$_{30–35}$), producing inulo-oligosaccharides (Fructose$_{3–5}$) and fructo-oligosaccharides (Glucose-Fructose$_{2–4}$) (*6*). Sequence comparison of EnIA with other members of GH32 using BLAST indicates that the enzyme consists of two domains: the N-terminal domain (residues 1–250) and the catalytic domain (residues 251–759) (Fig. 1A). It is the catalytic domain that displays an extensive amino acid sequence homology and identity among members of family GH32, including three putative catalytic residues (*7–11*). Except for crystallization reports of exoinulinases from *Aspergillus awamori* (*12*) and *Geobacillus stearothermophilus* KP1289 (*13*), little structural information had been available for members of family GH32 until the crystal structure of invertase from *Thermotoga maritima* was recently determined (*14*). Although the invertase belongs to GH32, its three-dimensional structure was notably shown to be similar to the β-propeller structures of glycosidase from families GH43, GH62, and GH68 (*14*, *15*). Specifically, invertase is composed of two individual modules: a five-bladed β-propeller catalytic module is linked to a C-terminal β-sandwich module. The novel structure of invertase revealed the location of three catalytic carboxylate residues in the cleft of the catalytic module as observed in other known structures of GH families, and will also serve as a framework of the enzyme mechanism of GH32.

Unlike the catalytic domain, the N-terminal domain of EnIA (NTD-EnIA) is not a sequence element common to the members of GH32 but present only in endoinulinases from *Arthrobacter* sp. S37 and *Pseudomonas mucidolence*, and in cycloinulo-oligosaccharide fructanotransferase (CFTase) from *Bacillus circulans* (*16*). Search using SMART (Simple Modular Architecture Research Tool) (*17*) classified the central region (residues 70–182) of NTD-EnIA as a "laminin-G like jelly-roll fold," a structural element found in functionally distant proteins such as CFTase from *Paenibacillus macerans* (Fig. 1B) (*18*).

In the present study, we investigated the possible roles of the unique NTD of EnIA in enzyme catalysis using mutagenesis and kinetic analysis, and found that this domain could serve as the functional and structural determinant to distinguish the enzyme from other members of the family GH32.

*To whom correspondence should be addressed. Su-Il Kim: Tel: +82-2-880-4643, Fax: +82-2-873-3112, E-mail: sikim@plaza.snu.ac.kr; Sangkee Rhee: Tel: +82-2-880-4647. Fax: +82-2-873-3112, E-mail: srheesnu@snu.ac.kr

(A)

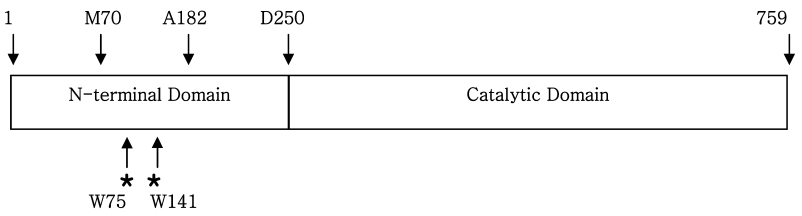

(B)

```
                75                                                  117
Ar       70-MTIQTWIALESYPSDSEQPYDALTPSSIIYQ-----RTNDAGFDIAINTYGEWWFTAHVGGQ-126
Bc      635-LTIEAWVAPRSY-----EWGDGNKLSAIVNQ---SDQDKAEGFALGMYRHGTWSLQAGIGGR-688
Pm      472-LTIEAWVAPRSY-----EWGDGNKLSAIVNQ---SDQDKAEGFSLGMYRHGTWSMQVGIGGQ-525
Ps       83-LTLEAWVAPRSY-----EWGDEQRLSAIVNQ---HDREKKEGFILGMYRHGTWSLQLGLDHE-136

           127      134        141
Ar      127-WRTVKAP--WL--FPL--YEWVQIAAVVDGDAGQLRLHLDDAAGPKVASVAIPTGSRFTQAA-182
Bc      689-W--IQA---WVNDHPLEKYKWNYVAATFDKEDGMMRLYLN---GEEVASQATPAG--------735
Pm      526-W--IQV---WVKDHPLEKYKWNYVAATFSKEDGKIKLYLN---GEEVASQATPVNVPIT----576
Ps      137-W--IEV---WSEDHPLPKNEWSYVVATYDKKTSMLKL--------------------------168
```

Fig. 1. **Schematic diagram of EnIA and its sequence comparison with other members of the jelly-roll fold.** (A) The unique N-terminal domain (residues 1–250) and the catalytic domain (residues 251–759) are indicated by arrows. A jelly-roll fold in the N-terminal domain spans from Met70 to Ala182. Highly conserved tryptophan residues among the homologous domains are indicated with asterisks. (B) The putative jelly-roll folds were searched using BLAST with residues 70–182 of EnIA (Ar) as a template, and then those amino acid sequences were aligned using CLUSTALW. Highly conserved tryptophan residues, namely, Trp75, Trp117, Trp127, Trp134, and Trp141, are numbered based on EnIA. Sequence identity from BLAST search was 34% and 31% for CFTase from *Bacillus circulans* (Bc) (*16*) and 31% for *Paenibacillus marcerans* (Pm) (*18*), respectively and 24% for endoinulinase from *Pseudomonas mucidolens* (Ps) [GenBank Accession number AAF24999].

MATERIALS AND METHODS

Construction of Mutant EnIAs—The *inu1* gene (GenBank accession number AJ131562) for EnIA was initially cloned into the pUC18 vector as reported previously (*19*), and later into the pRSET C vector (Invitrogen, Netherlands). The resulting plasmid pRIN24 harboring a gene for EnIA was used as a template for further site-directed mutagensis and the N-terminal truncation mutants. The plasmid pRIN24 contains a sequence for the N-terminal His-tag, the native protein in the *Bam*HI/*Hin*dIII fragment and an intrinsic *Sma*I site in the middle of the gene. Sequences for the series of N-terminal truncated EnIAs were amplified by PCR using primers flanking the 5′-end *Bam*HI site for the forward direction and *Sma*I site for the reverse direction. The sequences for primers are as follows: forward primer for Δ15 (5′-GGATCC-CCAACGGGTCGACCACGGTC-3′; *Bam*HI site is underlined), for Δ45 (5′-GGATCCGCGGGAACGCCTTCCGCAC-3′), for Δ70 (5′-GGATCCCGCAGATGACCATCCAGACCTG-3′), for Δ123 (5′-GGATCCACGTGGGTGGTCAGTGGCG-3′), for Δ182 (5′-GGATCCCTGCCGGCGCGCCGCTGG-3′), for Δ250 (5′-GGATCCGGTTCGCCGACGACATCCT-GCG-3′), and the common reverse primer (5′-CGTGATG-CCCGGGTCGAAGG-3′; *Sma*I is underlined). Each PCR product for the *Bam*HI/*Sma*I fragments was ligated into the pGEM-T easy vector (Promega, USA) and its sequence was confirmed. The resulting *Bam*HI/*Sma*I fragment was substituted for the corresponding fragment in the pRIN24 vector, generating various vectors for the truncated EnIA.

Sequences for W141A and W141K mutants were generated with QuikChange™ Site-Directed Mutagenesis Kit (Stratagene, USA). Two complementary oligonucleotides for each mutant were synthesized: 5′-GTTCCC-CCTGTACGAGGCGGTGCAGATTGCCGCCG-3′ and 5′-CGGCGGCAATCTGCACCGCCTCGTACAGGGGGAAC-3′ for the W141A mutant, 5′-GTTCCCCCTGTACGAGAAA-GTGCAGATTGCCGCCG-3′ and 5′-CGGCGGCAATCT-GCACTTTCTCGTACAGGGGGAAC-3′ for the W141K mutant (underlined nucleotides are codons for mutated residues). PCR-amplification followed by treatment with the restriction enzyme *Dpn*I selectively degraded the methylated parental pRIN24 template. The resulting PCR products containing a designed mutation were transfected into XL1-Blue supercompetent cells and the selected plasmids were sequenced.

W75A and W75K mutants were constructed by a megaprimer approach (*20*, *21*). First PCR was carried out to generate a megaprimer using mutagenic primers for W75A (5′-CCAGGGCGATCGCGGTCTGGATGG-3′; underlined sequence for alanine), W75K (5′-CCAGGGCGAT-TTTGGTCTGGATGG-3′; underlined sequence for lysine), and the flanking *Bam*HI site primer (5′-GGATCCCC-GCCACCGGTGACCCCGTC-3′). Megaprimers produced by the first PCR were purified and used in the second PCR with the intrinsic *Sma*I site primer (5′-CGTGATG-CCCGGGTCGAAGG-3′). The resulting *Bam*HI/*Sma*I fragments from the second PCR were then ligated into the pGEM-T easy vector and sequenced to verify the introduced mutations before replacing the corresponding fragments in the pRIN24 vector.

Construction of Chimeric Exoinulinase—The *exo1* gene (GenBank accession number AF366292) for an exoinulinase from *Bacillus* sp. snu-7 (ExIB), including a putative N-terminal secretion signal sequence, was cloned previously into a pBluescript SK(–) vector (Stratagene, USA). Later, the pRSET B–based pREX12 harboring native ExIB was constructed in the *Bam*HI/*Hin*dIII sites and used as the template for further gene manipulation (*22*).

Chimeric ExIB, where the NTD-EnIA was fused to the N-terminus of the native exoinulinase, was constructed by the following procedures. First, the DNA sequence for the NTD-EnIA in the pRIN24 vector described above was amplified using PCR with a forward primer flanking the 5′-end *Bam*HI site (5′-GGATCCCGCCACCGGTGAC-

CCC-3′; *Bam*HI site is underlined) and a reverse primer flanking the 5′-end *Xho*I site (5′-CTCGAGGGCGAACCG-CAGCCG-3′; *Xho*I site is underlined). Secondly, the 790-bp sequence from the N-terminus to the intrinsic *Bgl*II site of ExIB was amplified using a forward (5′-CTC-GAGCCCACCATGCGGCCAATAC-3′; *Xho*I site is underlined) and a reverse primer (5′-AGATCTACGTTCCC-GTCGG-3′; *Bgl*II site is underlined). The resulting PCR products for the NTD-EnIA (*Bam*HI/*Xho*I) and ExIB (*Xho*I/*Bgl*II) were respectively ligated into the pGEM-T easy vector and sequenced. The recombinant plasmid for the NTD-EnIA was digested with *Xho*I and *Nco*I at the upstream of *Bam*HI and *Xho*I. The purified *Nco*I/*Xho*I digest bearing a *Bam*HI/*Xho*I fragment was then inserted into the corresponding sites in the recombinant plasmid for ExIB. The resulting pGEM-T easy vector contained the *Bam*HI/*Bgl*II fragment for the NTD-EnIA and a segment of the N-terminal ExIB. The purified *Bam*HI/*Bgl*II fragment was then substituted for the corresponding sites of the pREX12 vector, producing the gene for chimeric ExIB.

Protein Expression, Purification and Enzyme Assay—Plasmids harboring the gene of interest were transformed and expressed as the fusion protein with a poly-histidine tag at the N-terminus. Specifically, each expression plasmid was transformed into heat-shocked $CaCl_2$-competent *E. coli* BL21 (DE3) pLysS. A 100-fold dilution of an overnight culture was made in Luria-Bertani media supplemented with 50 μg/ml of ampicillin and 35 μg/ml of chloramphenicol. The culture was grown at 37°C until absorbance at 600 nm reached 1.0, then isopropyl-1-thio-β-D-galactopyranoside was added to a final concentration of 1 mM. After further incubation for 6 h at 23°C, the cells were harvested by centrifugation at 4°C. The cell pellet was resuspended in buffer (20 mM sodium phosphate, pH 7.5, 500 mM NaCl), lyzed with lysozyme (final concentration of 1 mg/ml) and sonicated. The crude cell lysate was then incubated for 30 min on ice with 20 μg/ml of DNase I to degrade chromosomal DNA. After centrifugation at 15,000 rpm at 4°C for 30 min, the supernatant was applied to a HiTrap™-chelating 1-ml FPLC column (Amersham Bioscience, Uppsala, Sweden) on an ÄKTA purification system. The column was charged with $CoCl_2$ prior to sample application and subsequently washed with 10 column volumes of binding buffer (20 mM sodium phosphate, pH 7.5, 500 mM NaCl) followed by 5 column volumes of elution buffer (20 mM sodium phosphate, pH 7.5, 500 mM NaCl, 500 mM imidazole). The N-terminal His-tagged EnIA was eluted at about 50 mM imidazole and appeared as a single major band on a SDS-PAGE with Coomassie Brilliant Blue staining. The purified EnIA from the Co-chelating column was thus used for biochemical assay without further purification. Protein concentration was determined by Bradford's method (*23*).

Steady-state kinetics was measured using a spectrophotometer (SmartSpec™ 3000, Bio-Rad, USA), and the enzyme activity was calculated as the amount of reducing sugar liberated by the dinitrosalicylic acid method (*24*). A total of 0.1 ml of substrate–enzyme mixture containing 0.1–4 mM inulin and purified EnIA (1 unit) in 50 mM Tris-HCl (pH 7.5) was incubated at 37°C, and the amount of reducing sugar liberated was measured at intervals after terminating the reaction with 0.1 ml of dinitrosalicylic acid reagent. For kinetic analysis, enzyme activities at various substrate concentrations were measured every minute for the first 5 min of reaction to determine the initial velocity. D-Fructose (2.8–11.1 mM) was used as a standard sugar. The kinetic parameters, K_m and V_{max}, of the native and mutated enzymes were determined on a Lineweaver-Burk plot. Units of enzyme activity are defined as micromoles of product released per minute. The reported k_{cat} and K_m in this study are the averaged values of at least three independent measurements.

Thin-Layer Chromatography—Thin-layer chromatography was carried out in a developing chamber, with a mixture of *n*-propanol, ethylacetate, and water (3:1:1, v/v) as developing solvent. Substrate inulin was incubated for 24 h with the enzyme under identical conditions for enzyme assay. Sugar spots were visualized by spraying urea-metaphosphoric acid reagent onto a dried plate and heating the plate at 120°C for 5 min (*25*).

Size Exclusion Chromatography—Size exclusion chromatography (SEC) was conducted with a Superdex™ 200 HR 10/30 column (1 cm × 30 cm) on the ÄKTA system. Elution buffer was identical to the solution used for the enzyme assay (50 mM Tris-HCl, pH 7.5). Each protein under investigation was dialyzed against elution buffer, then loaded on the column at a flow rate of 0.5 ml/min. The collected peak fractions were analyzed by SDS-PAGE. In order to identify whether dimerization could occur as a result of reaction with a substrate, monomeric EnIA from SEC was reacted with 1 mM inulin for various periods (10 min, 60 min, and 24 h) at 37°C, then subjected to size-exclusion chromatography.

Table 1. **Kinetic parameters of the mutated and truncated EnIA.**[a]

	k_{cat} (min^{-1})	K_m (mM)	k_{cat}/K_m (min^{-1} mM^{-1})	Relative enzyme efficiency (%)
Native	$(4.27 \pm 0.38) \times 10^4$	0.33 ± 0.03	$(1.28 \pm 0.08) \times 10^5$	100
Δ15[b]	$(7.63 \pm 1.95) \times 10^2$	5.30 ± 1.67	$(1.46 \pm 0.11) \times 10^2$	0.11
Δ45[b,c]	N.D.	N.D.	N.D.	N.D.
Δ70[b,c]	N.D.	N.D.	N.D.	N.D.
Δ250[b,c]	N.D.	N.D.	N.D.	N.D.
W75A	$(2.41 \pm 0.02) \times 10^4$	0.35 ± 0.003	$(6.81 \pm 0.13) \times 10^4$	53.2
W75K	$(2.11 \pm 0.28) \times 10^3$	0.62 ± 0.01	$(3.95 \pm 1.19) \times 10^3$	3.1
W141A	$(2.88 \pm 0.19) \times 10^3$	0.42 ± 0.03	$(6.90 \pm 0.01) \times 10^3$	5.4
W141K	$(2.12 \pm 0.25) \times 10^2$	4.67 ± 0.07	$(0.45 \pm 0.05) \times 10^2$	0.035

[a]Molecular masses of mutated, truncated, and native EnIAs were calculated for the monomeric forms. [b]Truncated mutants are represented by the number of amino acid residues deleted from residue 1 of the N-terminal domain. [c]Enzyme was inactive to the substrate inulin and therefore kinetic parameters were not evaluated.

RESULTS

Truncated EnIA by the N-Terminal Domain—Most endoinulinases from various sources lack the N-terminal domain that is found in EnIA, and therefore the role of NTD was evaluated by constructing several N-terminal truncated mutants, including Δ250, Δ70, Δ123 and Δ182 (*i.e.*, deletion from N-terminus to the designated residue No.). In particular, Δ250 contains only the catalytic domain, having the whole NTD deleted, Δ123 disrupts the laminin-G like jelly-roll fold, and Δ182 has a partial NTD domain and the catalytic domain (Fig. 1A). Additional mutants, Δ15 and Δ45, were constructed to assess whether the structural integrity of NTD affects the enzyme function. Table 1 lists kinetic properties of these deletion mutants. Surprisingly, Δ250 EnIA did not have any detectable enzyme activity toward inulin, suggesting a possible linkage of the NTD-EnIA to catalysis. Δ250 EnIA was expressed as a soluble protein, though at a lower level than the native EnIA. Circular dichroism spectra for the native and Δ250 EnIAs were almost superimposable on each other, eliminating a possible protein-folding problem in the Δ250 enzyme (data not shown). Substrate affinity and the enzyme efficiency of Δ15 EnIA decreased by 16- and 883-fold, respectively, compared to those of the native EnIA. Other truncated EnIAs, Δ45, and Δ70, resulted in essentially inactive enzymes (Table 1). Moreover, partial or complete deletion of the jelly-roll fold as in the Δ123 and Δ182 mutants produced the enzymes as inclusion bodies, and their properties were not properly evaluated. These observations suggest that NTD-EnIA is related to catalysis and that the structural integrity of whole N-terminal domain is essential for enzyme catalysis in EnIA.

Role of the N-Terminal Domain in Enzyme Assembly—The requirement of structural integrity for the NTD-EnIA in catalysis provided a clue to the putative role of this unique domain in enzyme assembly. Figure 2 shows chromatograms of SEC under identical conditions for enzyme assay and determination of the apparent molecular mass of various enzymes constructed in this study. Interestingly, the elution profile of the native EnIA (solid line in Fig. 2A) exhibited two separable peaks: a peak marked open triangles (V_e = 11.5 ml) with an apparent molecular mass of 141 kDa, and a peak marked solid triangles (V_e = 13 ml) with an apparent molecular mass of 74 kDa. Each of these two independent peaks contained a single protein of 80 kDa on a SDS-PAGE, the theoretical monomeric molecular mass of the EnIA (inset in Fig. 2A). Therefore, these two peaks are thought to correspond to dimeric (open triangles) and monomeric (solid triangles) EnIA. Each of these EnIAs showed enzymatic activity toward inulin (Table 2). Specifically, the K_m value of the dimeric form is almost half that of the monomeric form, and therefore the dimeric enzyme showed 2-fold higher enzyme efficiency relative to the monomeric form. Transition between monomer and dimer appears to be extremely slow under our experimental conditions and

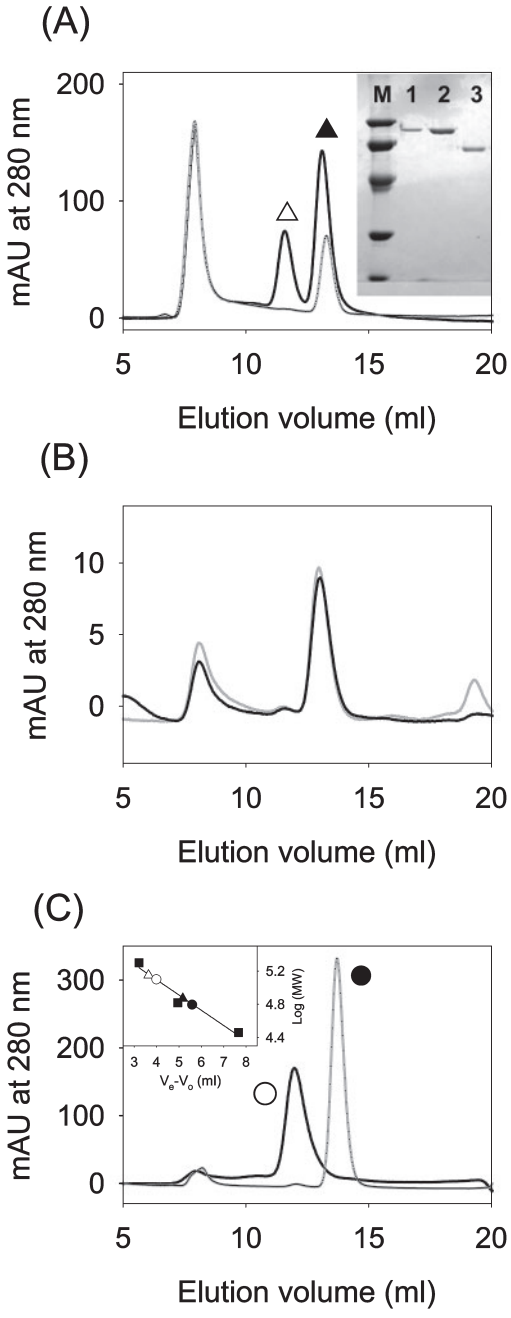

Fig. 2. **Size-exclusion chromatograms and SDS-PAGE of EnIA, Δ250, chimeric ExIB and ExIB.** (A) Two chromatograms are superimposed, showing the elution profiles of native EnIA as a solid line and Δ250 EnIA as a gray line. The elution peak for Blue dextran appears at an elution volume of about 8 ml. The inset shows SDS-PAGE of each elution peak: M, molecular weight markers; lane 1, peak (open triangles) of the native EnIA; lane 2, peak (solid triangles) of the native EnIA; lane 3, peak of the Δ250 EnIA. The concentration of EnIA and Δ250 EnIA was 0.20 mg/ml and 0.08 mg/ml, respectively. (B) Two chromatograms are superimposed, showing the elution profiles of native monomeric EnIA before (solid line) and after reaction (gray line). Monomeric EnIA in (A) was reacted with 1 mM inulin for 10 min at 37°C, then subjected to SEC. (C) Two chromatograms are superimposed, showing the elution profiles of chimeric ExIB as a solid line (open circles) and the native ExIB as a gray line (solid circles). Elution peak for Blue dextran is shown at an elution volume of about 8 ml. The inset shows the plot used to calculate the apparent molecular mass of the enzyme, where standard proteins are indicated with the filled squares (solid squares) for β-amylase (200 kDa), bovine serum albumin (66 kDa), and carbonic anhydrase (29 kDa).

Table 2. **Measured kinetic parameters of monomer and dimer of EnIA purified by size exclusion chromatography.**

Protein	k_{cat} (min^{-1})	K_m (mM)	k_{cat}/K_m (min^{-1} mM^{-1})
EnIA[a]	$(4.27 \pm 0.38) \times 10^4$	0.33 ± 0.03	$(1.28 \pm 0.08) \times 10^5$
Monomer	$(2.79 \pm 0.57) \times 10^4$	0.55 ± 0.11	$(5.08 \pm 0.01) \times 10^4$
Dimer	$(3.44 \pm 0.08) \times 10^4$	0.29 ± 0.05	$(1.20 \pm 0.17) \times 10^5$

[a]The molecular mass is calculated for the monomer.

insensitive to the presence of substrate. Figure 2B shows chromatograms of SEC for monomeric EnIA in the absence of inulin and after incubation with inulin for 10 min. The identical elution profile was also observed after extended incubation for 24 h with inulin, suggesting that dimerization has not occurred within the given time in the presence of 1 mM inulin. These results are consistent with the observation that there was no indication of transition between monomer and dimer after one month of storage of the EnIA at 4°C. Unlike the native enzyme, a truncated enzyme Δ250 (gray line in Fig. 2A) showed only a single peak at an elution volume of 13.2 ml with an apparent molecular mass of about 69 kDa, corresponding to a monomeric enzyme. When the truncated enzyme Δ70 was analyzed by SEC, both monomeric and dimeric peaks of Δ70 mutant were observed (data not shown). These results suggest that the 250 residues of NTD-EnIA are involved in dimerization.

The NTD-EnIA–mediated dimerization was undoubtedly observed in the chimeric ExIB. Native and chimeric forms of ExIB each eluted as a single peak, corresponding to a monomer (gray line, solid circles; V_e = 14 ml) and a dimer (solid line, open circles; V_e = 12 ml), respectively (Fig. 2C). Apparent molecular mass was estimated to be 129 kDa for the chimeric ExIB and 62 kDa for the native ExIB. Subsequently SDS-PAGE analysis confirmed that the chimeric ExIB forms a homodimer, demonstrating that the NTD-EnIA mediates the dimerization of the chimeric ExIB.

Enzymatic Properties of Chimeric ExIB—Evaluation of the kinetic parameters listed in Table 1 was complicated by the presence of both monomeric and dimeric forms of EnIA under the enzyme assay conditions. The role of the NTD-EnIA in catalysis was thus further investigated using the native and chimeric forms of ExIB, which are exclusively monomeric or dimeric, respectively. Figure 3 shows a thin-layer chromatogram of reaction products generated by native ExIB, native EnIA and chimeric ExIB from inulin as a substrate. EnIA (lane 4) and ExIB (lane 3) differ in their reaction specificity, the former producing oligomeric fructoses (F_3–F_5) and the latter a monomeric fructose (F_1). Chimeric ExIB (lane 5) maintained ExIB's activity and specificity, producing a monomeric fructose (F_1) identical to the native ExIB. These results suggest that the introduced NTD-EnIA did not cause global changes in function of ExIB. Table 3 lists the kinetic parameters of the native and chimeric ExIB. ExIB is known to have both exoinulinase and invertase activities, and these were independently assayed toward polymeric carbohydrate inulin for the exoinulinase activity and disaccharide sucrose for the invertase activity. Presence of the extra 250-residues in chimeric ExIB changed the optimal pH from 7.0 to 5.5, and both exoinulinase and invertase activities of chimeric ExIB

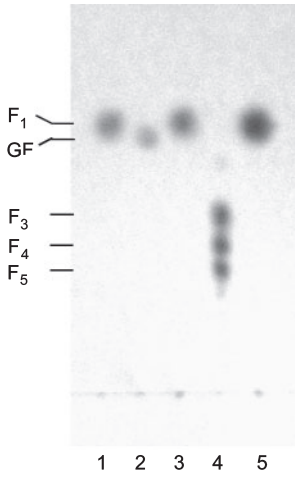

Fig. 3. **Thin-layer chromatogram of reaction products from ExIB, EnIA and chimeric ExIB.** Lanes 1 and 2 contain a monomeric fructose (F_1) and sucrose (GF) as standards, respectively. Reaction products from native ExIB (lane 3), native EnIA (lane 4) and chimeric ExIB (lane 5) were prepared and developed as described in "EXPERIMENTAL PROCEDURES." A trimeric (F_3), a tetrameric (F_4), and a pentameric (F_5) fructose were observed in lane 4.

were measured at pH 5.5. Chimeric ExIB showed a 2.6–7.9-fold increase in K_m and a concurrent 7.6–38.6-fold increase in k_{cat} relative to the native ExIB. Substrate preferences of the native and chimeric ExIB also differed. The I/S ratio, the relative enzyme efficiency toward inulin and sucrose, was about 0.75 for the native ExIB, but increased to 1.24 for the chimeric ExIB, indicating that the chimeric ExIB prefers the relatively large substrate inulin to sucrose.

Site-Directed Mutagenesis of Conserved Tryptophan Residues in the N-Terminal Domain—The putative function of the NTD-EnIA was further investigated using site-directed mutagenesis. Three-dimensional structures of several CBDs (carbohydrate-binding domains) indicated that aromatic residues play a pivotal role in ligand binding through hydrophobic stacking interaction (*26–28*). Sequence comparisons among the laminin-G like jelly-roll folds revealed five highly conserved tryptophan residues within the NTD-EnIA (Fig. 1B). Two of these residues, Trp75 and Trp141, were selected and then mutated to either the less bulky side chain alanine or the positively charged residue lysine. Measured kinetic parameters of these mutated EnIAs are listed in Table 1. Among four mutants (W75A, W75K, W141A, W141K), W75A mutant exhibited identical K_m but almost 2-fold reduction in k_{cat}, showing 53% of enzyme efficiency relative to the native EnIA. In W141A mutant, K_m and k_{cat} values were 27% higher and 15-fold lower than those of the native EnIA, resulting in significant reduction of enzyme efficiency to 5.4% of the native enzyme. Significant changes in kinetic parameters were observed in both W75K and W141K mutants, where replacement of tryptophan with lysine produced an almost inactive enzyme with activity and efficiency of 3.1% and 0.035%, respectively, relative to the native enzyme. Although we evaluated only two of five conserved tryptophan residues in the jelly-roll folds, our observations suggest that

Table 3. **Measured kinetic parameters of the native and chimeric ExIB toward inulin and sucrose.**

Protein sbstrates	k_{cat} (min^{-1})	K_m (mM)	k_{cat}/K_m (min^{-1} mM^{-1})	I/S ratio $(k_{cat}/K_m)_{inulin}/(k_{cat}/K_m)_{sucrose}$
ExIB				0.75
Inulin[a]	$(0.36 \pm 0.02) \times 10^3$	2.28 ± 0.08	$(1.57 \pm 0.03) \times 10^2$	
Sucrose[b]	$(4.62 \pm 0.22) \times 10^3$	22.02 ± 0.41	$(2.10 \pm 0.12) \times 10^2$	
Chimeric ExIB				1.24
Inulin[a]	$(1.39 \pm 0.05) \times 10^4$	18.03 ± 1.02	$(7.70 \pm 0.18) \times 10^2$	
Sucrose[b]	$(3.52 \pm 0.37) \times 10^4$	56.75 ± 7.42	$(6.22 \pm 0.15) \times 10^2$	

[a]Inulin concentration was in the range of 0.5–12 mM for ExIB, and of 2–40 mM for chimeric ExIB. [b]Sucrose concentration was in the range of 10–300 mM for both enzymes.

tryptophan residues in the NTD-EnIA are related to catalysis in EnIA.

DISCUSSION

Various mutational, kinetic and chromatographic results reported here provide evidence that NTD-EnIA performs pivotal roles in catalysis. One of these roles may be the formation of a dimer. Comparisons of the native and chimeric ExIB in chromatographic properties (Fig. 2C) revealed that the newly introduced NTD-EnIA in the chimeric ExIB mediates its dimerization. This proposed role of the NTD-EnIA was reinforced in the Δ250 EnIA, where the enzyme exists exclusively as a monomer (Fig. 2A) but was not supported by the observation that the native EnIA remains as a mixture of monomer and dimer. Although chimeric ExIB showed a dimeric and a monomeric peak of SEC at protein concentration as low as 0.005–0.01 mg/ml, only the dimeric chimeric ExIB was observed at higher concentration under our experimental conditions (data not shown). At this stage, we could not identify what kinds of factors are involved in the monomer–dimer equilibrium; it is highly possible that crucial factor(s) such as pH or salt are still missing or not optimized for dimerization. However, the transition between monomer and dimer must be such a slow process that a stable dimer is not generated even in the presence of the substrate (Fig. 2B). Our observations that various N-terminal truncated EnIAs were catalytically inactive (Table 1) and a chimeric enzyme exhibited higher enzyme efficiency toward large substrate inulin (Table 3) strongly suggest that the NTD-EnIA mediates the formation of a dimer, which optimizes its conformation for hydrolyzing inulin. Substrate-induced dimerization is known for diverse proteins. For example, human ribonuclease L, an interferon-inducible enzyme, exists as a monomer but is dimerized in the presence of 2′,5′-linked oligoadenylates (*29*). Phospholipase A_2 from *Bungarus caeruleus* was crystallized as a carbohydrate-induced homodimer for the first time, and the complex was caused by mannoses (*30*).

Besides the general role of NTD-EnIA in dimerization, tryptophan residues in the jelly-roll fold are involved in catalysis. In the absence of structural information about the NTD, we identified five conserved tryptophan residues within the jelly-roll fold (Fig. 1B). Initial mutational studies indicated that Trp141 is intimately related to catalysis based on the significant reduction in enzyme efficiency of W141A but not W75A (Table 1). In general, invariant or highly conserved aromatic side chains are localized in the CBD and are known to mediate hydrophobic stacking interactions with substrate *via* solvent-mediated and direct hydrogen bonds (*26–28*). Specifically, in the crystal structure of *Pseudomonas cellulosa* xylanase Xyn10C, Trp171 and Trp186 in the CBD form hydrophobic stacking interactions with xylose residues (*26*). Furthermore, Notenboom *et al.* showed that CBM9-2 from *Thermotoga maritima* xylanase 10A binds the reducing end of ligand with a complex hydrogen-bonding network involving mainly charged residues, as well as stacking interactions by Trp175 and Trp71 (*27*). These structural features were also visualized in the active site of invertase, where one molecule of glycerol used as a cryo-protectant bound to the active site, mimicking the fructose moiety in the substrate binding site with the nearby hydrophobic residues Trp41, Trp260 and Phe240 orientated toward the bound glycerol (*14*). It is known that mutation of the substrate-binding tryptophan residues causes a large decrease in the affinity for the substrate, in the range of 3- to 480-fold (*28*, *31*, *32*). But in the case of NTD-EnIA, W141A mutant showed only 27% increase in K_m value but significant reduction in enzyme efficiency (k_{cat}/K_m) by 18.5-fold, suggesting that W141 is not directly involved in carbohydrate binding but intimately related to enzyme catalysis. Our results provide evidence that the structural integrity of NTD-EnIA is crucial for enzyme catalysis.

From the structure and sequence of *T. maritima* invertase, Alberto *et al.* suggested that all family GH32 members contain the C-terminal β-sandwich module, which might play an important role in carbohydrate binding (*14*). The presence of a CBD at the C-terminus is not an isolated example but was observed in other families, including the α-amylase family (GH13) (*33*) and *T. maritima* xylanase 10A (*27*). Taken together, these results suggest that both the C-terminal β-sandwich module and the N-terminal domain in EnIA may regulate the recognition and binding of carbohydrate.

This report has shown that the unique NTD-EnIA domain is intimately involved in enzyme reactions, including dimerization and enzyme catalysis. Through mutagenesis and kinetic analysis, we have identified a putative domain involved in enzyme catalysis, but we have to wait for structural information to explain how the NTD-EnIA domain collectively coordinates these multiple roles in the enzyme reaction.

This work was supported by the Brain Korea 21 project, Korea Research Foundation Grant (KRF-2004-005-F00055), and by a grant (CG2114) from Crop Functional Genomics Center of the 21st Century Frontier Research Program funded by the Ministry of Science and Technology, Republic of Korea.

REFERENCES

1. Ly, H.D. and Withers, S.G. (1999) Mutagenesis of glycosidases. *Annu. Rev. Biochem.* **68**, 487–522
2. Henrissat, B. and Bairoch, A. (1993) New families in the classification of glycosyl hydrolases based on amino acid sequence similarities. *Biochem. J.* **293**, 781–788
3. Henrissat, B. and Bairoch, A. (1996) Updating the sequence-based classification of glycosyl hydrolases. *Biochem. J.* **316**, 695–696
4. Henrissat, B. and Davies, D. (1997) Structural and sequence-based classification of glycoside hydrolases. *Curr. Opin. Struct. Biol.* **7**, 637–644
5. Coutinho, P.M. and Henrissat, B. (1999) Carbohydrate-active enzymes server, http://afmb.cnrs-mrs.fr/~cazy/CAZY/index.html
6. Kang, S.-I., Chang, Y.-J., Oh, S.-J., and Kim, S.-I. (1998) Purification and properties of an endo-inulinase from an *Arthrobacter* sp. *Biotechnol. Lett.* **20**, 983–986
7. Reddy, A. and Maley, F. (1990) Identification of an active-site residue in yeast invertase by affinity labeling and site-directed mutagenesis. *J. Biol. Chem.* **265**, 10817–10820
8. Reddy, A. and Maley, F. (1996) Studies on identifying the catalytic role of Glu-204 in the active site of yeast invertase. *J. Biol. Chem.* **271**, 13953–13958
9. Pons, T., Olmea, O., Chinea, G., Beldarraín, A., Márquez, G., Acosta, N., Rodríguez, L., and Valencia, A. (1998) Structural model for family 32 of glycosyl-hydrolase enzymes. *Proteins* **33**, 383–395
10. Batista, F.R., Hernández, L., Fernández, J.R., Arrieta, J., Menéndez, C., Gómez, R., Támbara, Y., and Pons, T. (1999) Substitution of Asp-309 by Asn in the Arg-Asp-Pro (RDP) motif of *Acetobacter diazotrophicus* levansucrase affects sucrose hydrolysis, but not enzyme specificity. *Biochem. J.* **337**, 503–506
11. Song, D.D. and Jacques, N.A. (1999) Mutation of aspartic acid residues in the fructosyltransferase of *Streptococcus salivarius* ATCC 25975. *Biochem. J.* **344**, 259–264
12. Arand, M., Golubev, A.M., Neto, J.R.B., Polikarpov, I., Wattiez, R., Korneeva, O.S., Eneyskaya, E.V., Kulminskaya, A.A., Shabalin, K.A., Shishliannikov, S.M., Chepurnaya, O.V., and Neustroev, K.N. (2002) Purification, characterization, gene cloning and preliminary X-ray data of the exo-inulinase from *Aspergillus awamori*. *Biochem. J.* **362**, 131–135
13. Tsujimoto, Y., Watanabe, A., Nakano, K., Watanabe, K., Matsui, H., Tsuji, K., Tsukihara, T., and Suzuki, Y. (2003) Gene cloning, expression, and crystallization of a thermostable exo-inulinase from *Geobacillus stearothermophilus* KP1289. *Appl. Microbiol. Biotechnol.* **62**, 180–185
14. Alberto, F., Bignon, C., Sulzenbacher, G., Henrissat, B., and Czjzek, M. (2004) The three-dimensional structure of invertase (beta-fructosidase) from *Thermotoga maritima* reveals a bimodular arrangement and an evolutionary relationship between retaining and inverting glycosidases. *J. Biol. Chem.* **279**, 18903–18910
15. Pons, T., Naumoff , D.G., Martínez-Fleites, C., and Hernández, L. (2004) Three acidic residues are at the active site of a β-propeller architecture in glycoside hydrolase families 32, 43, 62, and 68. *Proteins* **54**, 424–432
16. Kanai, T., Ueki, N., Kawaguchi, T., Teranishi, Y., Atomi, H., Tomorbaatar, C., Ueda, M., and Tanaka, A. (1997) Recombinant thermostable cycloinulo-oligosaccharide fructanotransferase produced by *Saccharomyces cerevisiae*. *Appl. Environ. Microbiol.* **63**, 4956–4960
17. Schultz, J., Corpley, R.R., Doerks, T., Pongting, C.P., and Bork, P. (2000) SMART: a web-based tool for the study of genetically mobile domains. *Nucleic Acids Res.* **28**, 231–234
18. Kim, H.-Y. and Choi, Y.-J. (2001) Molecular characterization of cycloinulooligosaccharide fructanotransferase from *Bacillus macerans*. *Appl. Environ. Microbiol.* **67**, 995–1000
19. Kang, S.-I. and Kim, S.-I. (1999) Molecular cloning and sequence analysis of an endo-inulinase gene from *Arthrobacter* sp. *Biotechnol. Lett.* **21**, 569–574
20. Kammann, M., Laufs, J., Schell, J., and Gronenborn, B. (1989) Rapid insertional mutagenesis of DNA by polymerase chain reaction (PCR). *Nucleic Acids Res.* **17**, 5404
21. Ke, S.H. and Madison, E.L. (1997) Rapid and efficient site-directed mutagenesis by single-tube 'megaprimer' PCR method. *Nucleic Acids Res.* **25**, 3371–3372
22. Kim, K.-Y., Koo, B.-S., and Kim, S.-I. (2004) Cloning, expression, and purification of exoinulinase from *Bacillus* sp. snu-7. *J. Microbiol. Biotechnol.* **14**, 344–349
23. Bradford, M.M. (1976) A rapid and sensitive method for the quantitation of microgram quantities of protein utilizing the principle of protein-dye binding. *Anal. Biochem.* **72**, 248–254
24. Sengupta, S., Jana, M.L., Sengupta, D., and Naskar, A.K. (2000) A note on the estimation of microbial glycosidase activities by dinitrosalicylic acid reagent. *Appl. Microbiol. Biotechnol.* **53**, 732–735
25. Ha, Y.-J. and Kim, S.-I. (1992) Purification and characterization of endoinulase from *Streptomyces* sp. S56. *Kor. J. Appl. Mircrobiol. Biotechnol.* **20**, 551–558
26. Szabó, L., Jamal, S., Xie, H., Charnock, S.J., Bolam, D.N., Gilbert, H.J., and Davies, G.J. (2001) Structure of a family 15 carbohydrate-binding module in complex with xylopentaose: evidence that xylan binds in an approximate 3-fold helical conformation. *J. Biol. Chem.* **276**, 49061–49065
27. Notenboom, V., Boraston, A.B., Kilburn, D.G., and Rose, D.R. (2001) Crystal structure of the family 9 carbohydrate-binding module from *Thermotoga maritima* xylanase 10A in native and ligand-bound forms. *Biochemistry* **40**, 6248–6256
28. Simpson, P.J., Xie, H., Bolam, D.N., Gilbert, H.J., and Williamson, M.P. (2000) The structural basis for the ligand specificity of family 2 carbohydrate-binding modules. *J. Biol. Chem.* **275**, 41137–41142
29. Dong, B. and Silverman, R.H. (1995) 2-5A-dependent RNase molecules dimerize during activation by 2-5A. *J. Biol. Chem.* **270**, 4133–4137
30. Singh, G., Gourinath, S., Sarvanan, K., Sharma, S., Bhanumathi, S., Betzel, Ch., Yadav, S., Srinivasan A., and Singh, T.P. (2005) Crystal structure of a carbohydrate induced homodimer of phosholipase A_2 from *Bungarus caeruleus* at 2.1 Å resolution. *J. Struct. Biol.* **149**, 264–272
31. Xie, H., Gilbert, H.J., Charnock, S.J., Davies, G.J., Williamson, M.P., Simpson, P.J., Raghothama, S., Fontes, C.M.G.A., Dias, F.M.V., Ferreira, L.M.A., and Bolam, D.N. (2001) Clostridium thermocellum Xyn10B carbohydrate-binding module 22-2: the role of conserved amino acids in ligand binding. *Biochemistry* **40**, 9167–9176
32. Guan, L., Hu, Y., and Kaback, R. (2003) Aromatic stacking in the sugar binding site of the lactose permease. *Biochemistry* **42**, 1377–1382
33. Janeček, Š., Svensson, B., and MacGregor, E.A. (2003) Relation between domain evolution, specificity, and taxonomy of the α-amylase family members containing a C-terminal starch-binding domain. *Eur. J. Biochem.* **270**, 635–645